PHYSICAL REVIEW D **93,** 016009 (2016)

Chiral phase transition in QED_3 at finite temperature and impurity potential

Pei-Lin Yin,[1] Wei Wei,[2] Hai-Xiao Xiao,[2] Hong-Tao Feng,[3] Xiao-Jun Liu,[1,*] and Hong-Shi Zong[2,4,†]

[1]*Key Laboratory of Modern Acoustics, MOE, Institute of Acoustics, and Department of Physics, Collaborative Innovation Center of Advanced Microstructures, Nanjing University, Nanjing 210093, China*

[2]*Department of Physics, Nanjing University, Nanjing 210093, China*

[3]*Department of Physics, Southeast University, Nanjing 211189, China*

[4]*Joint Center for Particle, Nuclear Physics and Cosmology, Nanjing 210093, China*

(Received 16 June 2015; revised manuscript received 1 December 2015; published 20 January 2016)

In a realistic interacting system described by $(2+1)$-dimensional quantum electrodynamics (QED_3), there is always a certain number of impurities by which fermions are scattered. In general, impurity scattering can generate a finite density of states at the Fermi level, which screens the temporal component of the gauge field. This effect is expected to weaken dynamical fermion mass generation. Within the Born approximation, by introducing a damping term in the energy component of the fermion propagator, the influences of finite temperature and impurity scattering on the chiral phase transition in QED_3 are investigated. Pursuing this aim, we solve the Dyson-Schwinger equations for the fermion and boson propagators to the leading order in $1/N_f$ expansion at zero frequency and then calculate the chiral condensate, the chiral susceptibility, and the thermal susceptibility within a range of the impurity scattering rates Γ and the numbers of fermion flavors N_f. It is found that impurity scattering leads to an obvious suppression of the dynamical fermion mass generation and critical temperature T_c.

DOI: 10.1103/PhysRevD.93.016009

I. INTRODUCTION

Quantum chromodynamics (QCD), which describes the interactions between quarks and gluons, is regarded as an important component of the Standard Model of particle physics. Dynamical chiral symmetry breaking (DCSB) and quark color confinement are two fundamental features of it. Research on the chiral and deconfinement phase transitions at a finite temperature and/or chemical potential is conducive to deepening our understanding of the nature as well of the early Universe and, thus, becomes one of the hot topics in today's theoretical calculations and experimental measurements. A great many studies have been done in this field [1–12]. It is commonly accepted that with the temperature and/or chemical potential increasing, strongly interacting matter will undergo a phase transition from the Nambu-Goldstone phase (often referred to as the Nambu phase, in which chiral symmetry is dynamically broken) to the Wigner phase (where the chiral symmetry is partially restored). However, because of the complicated non-Abelian feature of QCD itself, it is difficult to have a thorough understanding of the mechanisms of DCSB and confinement. In this case, to gain a valuable comprehension of them, it is very suggestive to study some models which are structurally much simpler than QCD while sharing the same basic nonperturbative phenomena.

As an effective model, quantum electrodynamics in $(2+1)$ dimensions (QED_3) has several nonperturbative features in common with QCD, such as asymptotic freedom [13–18], DCSB [19–31], and confinement [32–36]. In addition, due to the coupling constant being dimensionful (its dimension is $\sqrt{\text{mass}}$), QED_3 is superrenormalizable and does not suffer from the ultraviolet divergences which are present in the corresponding four-dimensional theories. These properties of QED_3 enable it to serve as a toy model of QCD.

In the past three decades, the chiral phase transition in QED_3 has aroused great interest and been investigated intensively. At zero temperature and chemical potential, to the leading order in $1/N_f$ expansion, Appelquist, Nash, and Wijewardhana [37] first solved the Dyson-Schwinger equation (DSE) for the fermion self-energy function and found that the chiral phase transition takes place only when the number of fermion flavors is less than a critical number of fermion flavors $N_f^c = 32/\pi^2$. After taking into account the next-to-leading-order corrections to the fermion wave-function renormalization function, Nash [38] then obtained $N_f^c = 128/3\pi^2$. Later, Maris [39] solved a set of coupled integral equations for the fermion wave-function renormalization function, the fermion self-energy function, and the boson vacuum polarization with a range of simplified fermion-boson vertices and arrived at $N_f^c \approx 3.3$. Recently, Fischer *et al.* [40] employed an ansatz satisfying the Ward-Takahashi identity for the fermion-boson vertex and found

*liuxiaojun@nju.edu.cn
†zonghs@nju.edu.cn

$N_f^c \approx 4$. In addition, Bashir *et al.* [41] established that QED_3 can possess N_f^c if, and only if, the fermion wave-function renormalization function and boson vacuum polarization are homogeneous functions at infrared momenta and argued that if N_f^c exists in QED_3, then its value is independent of the gauge parameter. Braun *et al.* [42] studied the many-flavor phase diagram of QED_3 by analyzing the RG fixed-point structure of the theory and found that the phase transition towards a chirally broken phase occurring at small flavor numbers could be separated from the quasiconformal phase at larger flavor numbers by an intermediate phase.

At finite temperature and zero chemical potential, to the leading order in $1/N_f$ expansion, by retaining only the temporal component of the boson propagator and ignoring all but the zero-frequency component of the boson momentum, Dorey and Mavromatos studied the dynamical fermion mass generation [43]. After including the contribution from the fermion wave-function renormalization function and taking into account the momentum dependence of the fermion self-energy function, Aitchison and Klein-Kreisler then restudied the problem of dynamical fermion mass generation [44]. Recently, in the same approximation framework, Feng *et al.* solved the DSE for the fermion self-energy function and found a critical temperature T_c, at which the system undergoes a phase transition from the Nambu phase into the Wigner phase [45]. Furthermore, Lo and Swanson analyzed the behavior of the theory at a finite temperature and investigated the chiral phase transition of the QED_3 at a finite temperature and density by computing the dressed fermion and boson propagators with full frequency dependence [46].

In addition, since the discovery of high-T_c superconductivity, QED_3 has attracted considerable interest from physicists. It is generally believed that QED_3 with N_f flavors of fermions can be regarded as a possible low-energy effective theory for strongly correlated electronic systems, such as high-T_c cuprate superconductors [47–53] and graphene [54,55]. In these realistic interacting systems, there is always a certain number of impurities (or defects), by which the fermions are scattered. Generally, impurity scattering has two important effects. First, it generates a finite density of states at the Fermi level, which screens the temporal component of the gauge field. This effect is expected to weaken the strength of the gauge interaction. Second, it produces a finite damping of fermion quantum states and, thus, reduces the time for fermions to interact with their antiparticles. These effects indicate that impurity scattering will have important effects on the dynamical fermion mass generation and the chiral phase transition.

As far as we know, however, the influences of impurity scattering on the chiral phase transition have rarely been investigated in the previous literature. The authors of Ref. [27] studied the effects of finite chemical potential and impurity scattering on dynamical fermion mass generation. By solving the DSE for the fermion self-energy function, they found that the finite chemical potential and impurity scattering lead to a strong suppression of the dynamical fermion mass generation and the critical number of fermion flavors N_f^c. As mentioned above, in the realistic applications of QED_3 to condensed matter physics, impurity scattering is usually important and, thus, should not be ignored. The purpose of this paper is to study the effects of impurity scattering on the chiral phase transition by solving the DSEs for the fermion and boson propagators to the leading order in $1/N_f$ expansion.

This paper is organized as follows: In Sec. II, we set up the DSEs satisfied by the scalar functions of propagators including impurity scattering. In Sec. III, the order parameter describing the chiral phase transition of the system is presented. In Sec. IV, we calculate the scalar functions of propagators and order parameter within a range of the impurity scattering rates Γ and the numbers of fermion flavors N_f and then discuss the relationship between the critical temperature T_c and the impurity scattering rate Γ. A brief summary and discussion are given in Sec. IV.

II. DYSON-SCHWINGER EQUATIONS IN THE PRESENCE OF IMPURITY SCATTERING

In Euclidean space, the Lagrangian density of QED_3 with N_f flavors of massless fermions is given by

$$\mathcal{L} = \sum_{f=1}^{N_f} \bar{\psi}_f (\not{\partial} + ie\not{A})\psi_f + \frac{1}{4}F_{\mu\nu}^2 + \frac{1}{2\xi}(\partial_\mu A_\mu)^2. \quad (1)$$

In $(2+1)$-dimensional space-time, the lowest rank irreducible representation of the Lorentz group is two-dimensional. In this representation, Dirac fermions are described by two-component spinors and the γ matrices may be chosen as the usual Pauli matrices. However, as the three Pauli matrices are a complete set of mutually anticommuting 2×2 matrices, it is impossible to define the other 2×2 matrix that anticommutes with all three γ matrices. Consequently, there is nothing to generate a chiral symmetry that would be broken by a mass term $m\bar{\psi}\psi$, whether it be explicit or dynamically generated. Besides, any mass term has the undesirable property that it is odd under parity transformations. Given these, we employ four-component spinors and a 4×4 matrix representation as in four-dimensional space-time in this paper. A more thorough discussion of the reducible and irreducible representations of the Dirac matrices in QED_3 can be seen in Refs. [56,57].

For the fermion propagator, the finite temperature version of DSE is given by

$$S^{-1}(p) = S_0^{-1}(p) + \Sigma(p), \quad (2)$$

$$S_0^{-1}(p) = i\vec{\gamma}\cdot\vec{p} + i\gamma_3 p_3, \tag{3}$$

$$\Sigma(p) = T\sum\!\!\!\!\!\!\int \gamma_\mu S(k)\Gamma_\nu(p,k)D_{\mu\nu}(q), \tag{4}$$

where $p = (p_3, \vec{p})$ with $p_3 = (2m+1)\pi T$ and $|\vec{p}| = P$, $k = (k_3, \vec{k})$ with $k_3 = (2n+1)\pi T$ and $|\vec{k}| = K$, and $q = (q_3, \vec{q}) = p - k$ with $q_3 = 2(m-n)\pi T$ and $|\vec{q}| = Q = |\vec{p} - \vec{k}|$. The notation $\sum\!\!\!\!\!\!\int$ denotes $\sum_{n=-\infty}^{+\infty}\int\frac{d^2\vec{k}}{(2\pi)^2}$. $S^{-1}(p)$ and $S_0^{-1}(p)$ are the inverse dressed and free fermion propagators, respectively, $\Sigma(p)$ is the fermion self-energy, $\Gamma_\nu(p,k)$ is the dressed fermion-boson vertex, and $D_{\mu\nu}(q)$ is the dressed boson propagator.

As we all know, the introduction of temperature to a system breaks the original O(3) symmetry to O(2). The most general form of the inverse dressed fermion propagator can be written as [58,59]

$$S^{-1}(p) = i\vec{\gamma}\cdot\vec{p}A(p) + B(p) + i\gamma_3 p_3 C(p) + \vec{\gamma}\cdot\vec{p}\gamma_3 p_3 D(p), \tag{5}$$

where $A(p)$ and $C(p)$ are usual fermion wave-function renormalization functions and $B(p)$ is the fermion self-energy function. Because the tensor term $\vec{\gamma}\cdot\vec{p}\gamma_3 p_3$ is not invariant under the time reversal transformation, the corresponding dressing function $D(p)$ vanishes exactly [60,61], and then the general form of the inverse dressed fermion propagator is

$$S^{-1}(p) = i\vec{\gamma}\cdot\vec{p}A(p) + i\gamma_3 p_3 C(p) + B(p). \tag{6}$$

To the leading order in $1/N_f$ expansion, we neglect the effect of the fermion wave-function renormalization functions $A(p)$ and $C(p)$ and replace the dressed vertex $\Gamma_\nu(p,k)$ by the bare one γ_ν. Such an approximation scheme is consistent with the requirement following from the Ward-Takahashi identity that the fermion wave-function renormalization function and the vertex renormalization are equal. In addition, the fermion self-energy function becomes frequency independent when the instantaneous exchange approximation [21,26,27,29,43,44,62–64] is employed for the boson propagator. Hereafter, the approximations will be kept for the fermion propagator. Substituting Eqs. (3), (4), and (6) into Eq. (2) and then taking the trace on both sides of this equation yields

$$B(P^2,T) = T\sum\!\!\!\!\!\!\int \frac{B(K^2,T)}{k_3^2 + K^2 + B^2(K^2,T)} D_{\mu\mu}(Q,T). \tag{7}$$

For the boson propagator, the finite temperature version of DSE is written as

$$D_{\mu\nu}^{-1}(q) = D_{\mu\nu}^{0,-1}(q) + \Pi_{\mu\nu}(q), \tag{8}$$

$$D_{\mu\nu}^{0,-1}(q) = q^2(\delta_{\mu\nu} - q_\mu q_\nu/q^2), \tag{9}$$

$$\Pi_{\mu\nu}(q) = -N_f T\sum\!\!\!\!\!\!\int \mathrm{Tr}[\gamma_\mu S(k)\Gamma_\nu(p,k)S(p)], \tag{10}$$

where $D_{\mu\nu}^{0,-1}(q)$ is the inverse free boson propagator and $\Pi_{\mu\nu}(q)$ is the vacuum polarization tensor. Herein we have chosen the Landau gauge.

As aforementioned, the introduction of temperature to a system breaks the original O(3) symmetry to O(2). In general, the vacuum polarization tensor has four independent components corresponding to the four independent O(2)-invariant tensors. However, as at $T = 0$ it satisfies the transversality condition and, thus, can be conveniently decomposed in terms of two independent transverse tensors [43]

$$\Pi_{\mu\nu}(q) = \Pi_A(q)A_{\mu\nu} + \Pi_B(q)B_{\mu\nu}, \tag{11}$$

where

$$A_{\mu\nu} = \left(\delta_{\mu 0} - \frac{q_\mu q_0}{q^2}\right)\frac{q^2}{Q^2}\left(\delta_{\nu 0} - \frac{q_\nu q_0}{q^2}\right) \tag{12}$$

and

$$B_{\mu\nu} = \delta_{\mu i}\left(\delta_{ij} - \frac{q_i q_j}{Q^2}\right)\delta_{j\nu}, \tag{13}$$

$A_{\mu\nu}$ and $B_{\mu\nu}$ are orthogonal and satisfy the following relationship:

$$A_{\mu\nu} + B_{\mu\nu} = \delta_{\mu\nu} - \frac{q_\mu q_\nu}{q^2}. \tag{14}$$

The functions $\Pi_A(q)$ and $\Pi_B(q)$ are related to the temporal and spatial components of the vacuum polarization tensor $\Pi_{\mu\nu}(q)$ by the following expressions:

$$\Pi_A(q) = \frac{q^2}{Q^2}\Pi_{00}(q) \tag{15}$$

and

$$\Pi_B(q) = \Pi_{ii}(q) - \frac{q_0^2}{Q^2}\Pi_{00}(q). \tag{16}$$

Substituting Eqs. (9) and (11) into Eq. (8), we can obtain the dressed finite temperature boson propagator

$$D_{\mu\nu}(q) = \frac{A_{\mu\nu}}{q^2 + \Pi_A(q)} + \frac{B_{\mu\nu}}{q^2 + \Pi_B(q)}. \tag{17}$$

Herein we shall follow Refs. [21,26,29,43,44,62] in retaining only the temporal component of the boson propagator

and ignoring all but the zero-frequency component of the boson momentum (instantaneous exchange approximation), and then we are left with

$$D_{\mu\nu}(Q,T)=\frac{2\delta_{\mu3}\delta_{\nu3}}{Q^2+\Pi(Q^2,T)}; \tag{18}$$

we will retain these approximations for the boson propagator in the following sections.

To the leading order in $1/N_f$ expansion, the one-loop contribution to the vacuum polarization tensor can be obtained by replacing the dressed fermion propagator and vertex with their bare quantity separately in Eq. (10):

$$\begin{aligned}\Pi_{\mu\nu}(q)&=-N_fT\sum\!\!\!\!\!\!\int \mathrm{Tr}[\gamma_\mu S_0(k)\gamma_\nu S_0(p)]\\&=4N_fT\int_0^1 dx\sum\!\!\!\!\!\!\int\frac{\mathcal{I}_{\mu\nu}}{[l^2+x(1-x)q^2]^2},\end{aligned} \tag{19}$$

where

$$\begin{aligned}\mathcal{I}_{\mu\nu}&=2l_\mu l_\nu+(1-2x)(l_\mu q_\nu+l_\nu q_\mu-l\cdot q\delta_{\mu\nu})\\&\quad+2x(1-x)(q^2\delta_{\mu\nu}-q_\mu q_\nu)-[l^2+x(1-x)q^2]\delta_{\mu\nu}\end{aligned} \tag{20}$$

and $l=k+xq$. The detailed calculations of the one-loop vacuum polarization tensor are presented in Appendix A.

The temporal component of the one-loop vacuum polarization tensor is given by

$$\begin{aligned}\Pi_{33}(q)&=4N_fT\int_0^1 dx\sum\!\!\!\!\!\!\int[S_1-2(L^2+x(1-x)q_0^2)S_2\\&\quad+(1-2x)q_0S^*],\end{aligned} \tag{21}$$

where

$$S_i=\sum_{n=-\infty}^{+\infty}\frac{1}{[l_0^2+L^2+x(1-x)q^2]^i} \tag{22}$$

and

$$S^*=\sum_{n=-\infty}^{+\infty}\frac{l_0}{[l_0^2+L^2+x(1-x)q^2]^2}. \tag{23}$$

Within the instantaneous exchange approximation, the integral in Eq. (21) can be performed by the methods presented in Ref. [43]. After a tedious but straightforward computation, we obtain the following expression for the polarization function:

$$\Pi(Q^2,T)=\frac{2N_fT}{\pi}\int_0^1 dx\ln\left[2\cosh\frac{\sqrt{x(1-x)}Q}{2T}\right]. \tag{24}$$

Combining Eqs. (7), (18), and (24), the fermion self-energy function can be numerically solved using the straightforward iteration method. Once the momentum dependence of the fermion self-energy function is obtained, we can further investigate the dynamical fermion mass generation and the chiral phase transition.

The discussions above can be generalized to the case of finite temperature and impurity scattering. Because the problem of impurity scattering is very complicated and now has not been fully understood, some approximations are required before progress can be made. If we consider a single impurity atom, then impurity scattering can be treated by the self-consistent Born approximation. Within this approximation, the retarded fermion propagator develops a finite imaginary part, which is usually represented by a constant scattering rate Γ [65]. To study the problem of impurity scattering, it is most convenient to work in the Matsubara formalism, and thus the inverse dressed and free fermion propagators are written as [27]

$$S^{-1}(p,\Gamma)=i\vec{\gamma}\cdot\vec{p}+i\gamma_3p_{3,\Gamma}+B(p,\Gamma), \tag{25}$$

$$S_0^{-1}(p,\Gamma)=i\vec{\gamma}\cdot\vec{p}+i\gamma_3p_{3,\Gamma}, \tag{26}$$

where $p_{3,\Gamma}=p_3+\Gamma\mathrm{sgn}(p_3)$. Intuitively, the parameter Γ measures the decaying rate of the fermion state characterized by such quantum numbers as $(p_3,\vec{p})$, which is known as the Landau damping effect.

Substituting Eqs. (4), (25), and (26) into Eq. (2) and taking the trace on both sides of this equation, we arrive at

$$\begin{aligned}B(P^2,T,\Gamma)&=T\sum\!\!\!\!\!\!\int\frac{B(K^2,T,\Gamma)}{k_{3,\Gamma}^2+K^2+B^2(K^2,T,\Gamma)}\\&\quad\times D_{\mu\mu}(Q,T,\Gamma).\end{aligned} \tag{27}$$

Analogizing the derivation of Eq. (18), the boson propagator in the presence of impurity scattering can be written as

$$D_{\mu\nu}(Q,T,\Gamma)=\frac{2\delta_{\mu3}\delta_{\nu3}}{Q^2+\Pi(Q^2,T,\Gamma)}, \tag{28}$$

where $\Pi(Q^2,T,\Gamma)$ is the polarization function including impurity scattering.

Substituting Eq. (26) into Eq. (10), the polarization function is expressed as

$$\Pi(Q^2,T,\Gamma)=\frac{4N_fT}{\pi}\int_0^1 dx\left\{\mathrm{Re}\left[\ln\Gamma\left(\frac{1}{2}+\frac{\Gamma+iX}{2\pi T}\right)\right]+\frac{X^2-C^2}{X^2}\mathrm{Im}\left[\psi\left(\frac{1}{2}+\frac{\Gamma+iX}{2\pi T}\right)\right]\right\}\Bigg|_C^\infty, \tag{29}$$

where $C=\sqrt{x(1-x)}Q$, $\Gamma(z)$ is the usual Gamma function, and $\psi(z)=\mathbf{\Gamma}'(z)/\mathbf{\Gamma}(z)$ is the Digamma function. The detailed calculations of the one-loop vacuum polarization tensor in the presence of impurity scattering are presented in Appendix B.

To simplify the theoretical and numerical analysis, we use the same approximate expressions for this two functions as that presented in Ref. [27]:

$$\mathrm{Re}\left[\ln\mathbf{\Gamma}\left(\frac{1}{2}+\frac{\Gamma+iX}{2\pi T}\right)\right]\approx-\frac{T+c\Gamma}{2T}\ln\left[\cosh\frac{X}{2(T+c\Gamma)}\right] \tag{30}$$

and

$$\mathrm{Im}\left[\psi\left(\frac{1}{2}+\frac{\Gamma+iX}{2\pi T}\right)\right]\approx\frac{\pi}{2}\tanh\frac{X}{2(T+c\Gamma)}, \tag{31}$$

where the constant $c=10^{\ln 2}/(2\pi)$. After substituting Eqs. (30) and (31) into Eq. (29) and performing some algebraic calculations, we arrive at

$$\Pi(Q^2,T,\Gamma)=\frac{2N_f(T+c\Gamma)}{\pi}\int_0^1 dx\ln\left[2\cosh\frac{\sqrt{x(1-x)}Q}{2(T+c\Gamma)}\right]. \tag{32}$$

From Eqs. (27), (28), and (32), the fermion self-energy function in the presence of impurity scattering can be obtained, and thus we can investigate the influences of impurity scattering on the dynamical fermion mass generation and the critical temperature T_c.

III. CRITERIA FOR CHIRAL PHASE TRANSITION

The chiral condensate is the vacuum expectation value for the scalar operator $\bar\psi\psi$. The character, the nonzero value of which indicates that chiral symmetry reflected on the Lagrangian level is spontaneously broken on the vacuum level and the chiral symmetry gets restored when the chiral condensate vanishes for the chiral limit, makes it possible to define the chiral condensate as the order parameter for the chiral phase transition.

The chiral condensate is commonly given by the first-order derivative of the generating functional with respect to the current mass of the fermion

$$\langle\bar\psi\psi\rangle(T)=-\frac{T}{V}\frac{\partial\ln Z}{\partial m}=-T\sum\!\!\!\!\!\!\int\mathrm{Tr}[S(p)], \tag{33}$$

where the notation Tr denotes the trace operation over Dirac indices of the fermion propagator.

In addition, dynamical properties of a many-particle system can be investigated by measuring the response of the system to an external perturbation that disturbs the system only slightly in its equilibrium state. A noticeable measure is the susceptibility that is defined as the first-order derivative of the order parameter with respect to the external field. The order parameter is radically different in two phases and thus characterizes the phase transition of the system. As a result, the divergence or some other singular behaviors of the susceptibility are usually regarded as essential characteristics of phase transition.

The first-order derivative of the chiral condensate with respect to the current mass of the fermion is known as the chiral susceptibility [66–68]:

$$\chi^c(T)=-\frac{\partial\langle\bar\psi\psi\rangle(T)}{\partial m}=\frac{T}{V}\frac{\partial^2\ln Z}{\partial m^2}. \tag{34}$$

It is known that the chiral susceptibility measures the response of the chiral condensate to a small perturbation of the current mass of the fermion from Eq. (34).

Similarly, the first-order derivative of the chiral condensate with respect to the temperature is referred to as thermal susceptibility [69–72]:

$$\chi^T(T)=\frac{\partial\langle\bar\psi\psi\rangle(T)}{\partial T}=-\frac{1}{V}\frac{\partial^2(T\ln Z)}{\partial T\partial m}. \tag{35}$$

We can analyze the behavior of the chiral condensate with varying temperature more directly from Eq. (35).

Equations (33)–(35) can be generalized to the case of finite temperature and impurity scattering by replacing the dressed fermion propagator with the one including impurity scattering:

$$\langle\bar\psi\psi\rangle(T,\Gamma)=-T\sum\!\!\!\!\!\!\int\mathrm{Tr}[S(p,\Gamma)], \tag{36}$$

$$\chi^c(T,\Gamma)=-\frac{\partial\langle\bar\psi\psi\rangle(T,\Gamma)}{\partial m}, \tag{37}$$

$$\chi^T(T,\Gamma)=\frac{\partial\langle\bar\psi\psi\rangle(T,\Gamma)}{\partial T}. \tag{38}$$

IV. NUMERICAL RESULTS

From the discussions mentioned above, we know that solving numerically Eq. (27) and thus obtaining the momentum dependence of the fermion self-energy function are needed, when we study the dynamical fermion mass generation and the chiral phase transition in the presence of

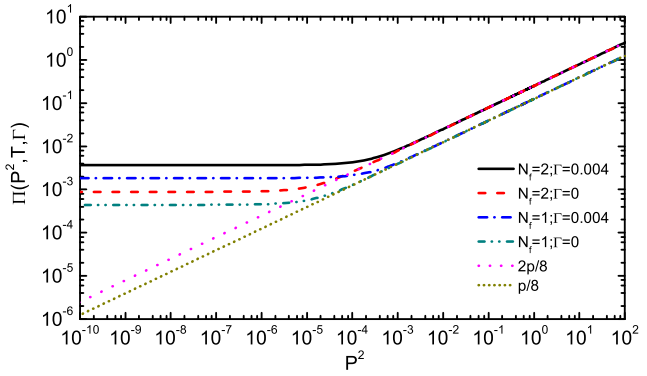

FIG. 1. Momentum dependence of the polarization function $\Pi(P^2, T, \Gamma)$ for different impurity scattering rates Γ and numbers of fermion flavors N_f at $T = 10^{-3}$.

impurity scattering. However, before doing this, it is necessary to investigate the momentum dependence of the polarization function. In the following discussion, we will first study the behavior of the polarization function.

Performing the integral over the parameter x in Eq. (32), we can know how the polarization function changes as a function of momentum. In Fig. 1, we show the momentum dependence of it for different impurity scattering rates Γ and numbers of fermion flavors N_f.

It can be seen that the polarization function is almost constant in the infrared region and reduces to the one-loop approximation result in the ultraviolet region. For a given number of fermion flavors N_f, the infrared constant value of the polarization function increases as the impurity scattering rate Γ changes from zero to a finite value, and the ultraviolet polarization functions for different impurity scattering rates Γ are all close to a common one-loop approximation result. When the number of fermion flavors N_f increases, the polarization function rises.

The infrared value of the polarization function can be obtained by taking the limit of the exchange momentum Q tending to zero:

$$\lim_{Q\to 0}\Pi(Q^2, T, \Gamma) = \frac{2\ln 2N_f}{\pi}(T + c\Gamma), \tag{39}$$

and the ultraviolet asymptotic behavior of the polarization function can also be obtained by the same method:

$$\lim_{Q\to\infty}\Pi(Q^2, T, \Gamma) = \frac{N_f Q}{8}. \tag{40}$$

Now we solve numerically the DSE of the fermion self-energy function. Using the following identity:

$$\sum_{n=-\infty}^{+\infty}\frac{1}{k_{3,\Gamma}^2 + \varepsilon_{K,T,\Gamma}^2} = \frac{1}{\pi T\varepsilon_{K,T,\Gamma}}\mathrm{Im}\left[\psi\left(\frac{1}{2} + \frac{\Gamma + i\varepsilon_{K,T,\Gamma}}{2\pi T}\right)\right], \tag{41}$$

where $\varepsilon_{K,T,\Gamma} = \sqrt{K^2 + B^2(K^2, T, \Gamma)}$, and then combining with Eq. (31), Eq. (27) reduces to

$$B(P^2, T, \Gamma) = \int\frac{\mathrm{d}^2K}{(2\pi)^2}\frac{B(K^2, T, \Gamma)}{\varepsilon_{K,T,\Gamma}}\tanh\frac{\varepsilon_{K,T,\Gamma}}{2(T + c\Gamma)} \times\frac{1}{[Q^2 + \Pi(Q^2, T, \Gamma)]}. \tag{42}$$

The equation can be solved by using the straightforward iteration method. In Fig. 2, we display the momentum dependence of the fermion self-energy function for different impurity scattering rates Γ and numbers of fermion flavors N_f.

We can clearly see that the fermion self-energy function is nearly constant in the infrared region and decreases monotonically to zero in the ultraviolet region. For a given number of fermion flavors N_f, the infrared constant value of the fermion self-energy function decreases as the impurity scattering rate Γ changes from zero to a finite value, and the ultraviolet fermion self-energy functions for different impurity scattering rates Γ are all close to zero. The fermion self-energy function also falls when the number of fermion flavors N_f increases.

For the chiral condensate, substituting Eq. (25) into Eq. (36) and performing the summation yield

$$\langle\bar{\psi}\psi\rangle(T, \Gamma) = -2\int\frac{\mathrm{d}^2P}{(2\pi)^2}\frac{B(P^2, T, \Gamma)}{\varepsilon_{P,T,\Gamma}}\tanh\frac{\varepsilon_{P,T,\Gamma}}{2(T + c\Gamma)}. \tag{43}$$

The chiral condensate can be calculated once the self-energy function is obtained by Eq. (42). The temperature dependence of it for different impurity scattering rates Γ and numbers of fermion flavors N_f is shown in Fig. 3.

We find that $-\langle\bar{\psi}\psi\rangle$, the negative of the chiral condensate, decreases slowly when the temperature is small and falls rapidly to zero as the temperature approaches to

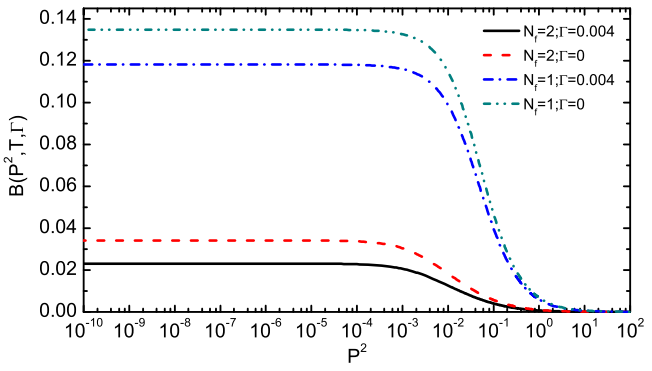

FIG. 2. Momentum dependence of the fermion self-energy function $B(P^2,\mathrm{T},\Gamma)$ for different impurity scattering rates Γ and numbers of fermion flavors N_f at $T = 10^{-3}$.

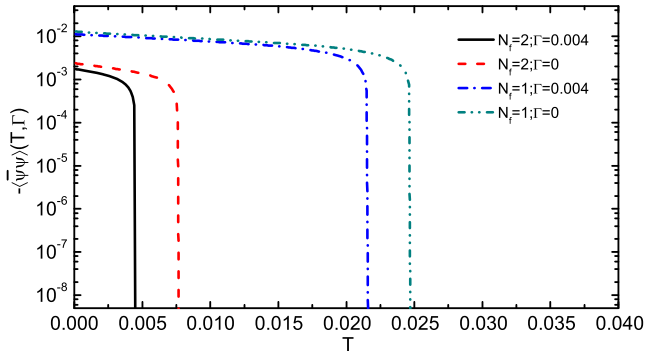

FIG. 3. Temperature dependence of $-\langle\bar{\psi}\psi\rangle(T,\Gamma)$ for different impurity scattering rates Γ and numbers of fermion flavors N_f.

the critical temperature T_c. For a given number of fermion flavors N_f, the critical temperature T_c decreases when the impurity scattering rate Γ changes from zero to a finite value, which shows that impurity scattering indeed suppresses the dynamical fermion mass generation. This is consistent with the discussions presented in the introduction. In addition, the critical temperature T_c also decreases as the number of fermion flavors N_f increases.

Here, we notice that, in the deep infrared limit, QED$_3$ at a finite temperature becomes an effectively two-dimensional theory in which there is no spontaneous breaking of a continuous symmetry due to the Coleman-Mermin-Wagner theorem [73,74]. As a consequence, there is only spontaneous chiral symmetry breaking in QED$_3$ in the zero-temperature limit. Nevertheless, in the large-N_f approximation, the long-range fluctuations are absent, and thus dynamical mass generation can still be observed even in two dimensions as is illustrated by the chirally symmetric Gross-Neveu model [75,76]. This can also be found in condensed matter physics, where dynamical chiral symmetry breaking is studied self-consistently in the framework of the mean field theory, which is the large-N_f approximation employed in the present studies. In such a theory, the correlation between fluctuations of the order parameter is ignored. The mean field transition temperature provides a correct energy scale below which the amplitude of the order parameter becomes finite and its spatial correlation becomes strong and rather long-ranged. In this sense, the mean field transition temperature marks a crossover in the thermodynamic properties. In particular, for a U(1) or O(2) symmetry to be broken, there is in fact an algebraic order below the so-called Kosterlitz-Thouless transition temperature, a temperature not far from the mean field one. Moreover, in a realistic layered system, the interlayer coupling can easily drive the system into a true ordered state once the in-plane correlations are already strong, e.g., below the mean field transition temperature. In this sense, the mean field transition temperature in two dimensions provides the upper limit in a layered three-dimensional system. In addition, in the context of high-temperature superconductivity, the chirally broken and symmetric phases of QED$_3$ are associated with the antiferromagnetic spin-density wave state and the pseudogap phase of the cuprates described as algebraic Fermi liquid, respectively [50,51]. It is commonly accepted that with the temperature and/or doping increasing, the cuprates will undergo a phase transition from the antiferromagnetic spin-density wave phase to the pseudogap phase.

For the chiral susceptibility, substituting Eq. (43) into Eq. (37) and performing the summation, then we arrive at

$$\chi^c(T,\Gamma) = 2\int\frac{d^2P}{(2\pi)^2}\left\{B_m(P^2,T,\Gamma)\left[\frac{P^2\tanh\frac{\varepsilon_{P,T,\Gamma}}{2(T+c\Gamma)}}{\varepsilon^3_{P,T,\Gamma}} + \frac{B^2(P^2,T,\Gamma)\mathrm{sech}^2\frac{\varepsilon_{P,T,\Gamma}}{2(T+c\Gamma)}}{2(T+c\Gamma)\varepsilon^2_{P,T,\Gamma}}\right] - \frac{\tanh\frac{P}{2T}}{P}\right\}, \quad (44)$$

where the function $B_m(P^2,T,\Gamma)$ is just the derivative of the fermion self-energy function with respect to the current mass and can be given by

$$B_m(P^2,T,\Gamma) = 1 + \int\frac{d^2K}{(2\pi)^2}\left\{\frac{K^2\tanh\frac{\varepsilon_{K,T,\Gamma}}{2(T+c\Gamma)}}{\varepsilon^3_{K,T,\Gamma}} + \frac{B^2(K^2,T,\Gamma)\mathrm{sech}^2\frac{\varepsilon_{K,T,\Gamma}}{2(T+c\Gamma)}}{2(T+c\Gamma)\varepsilon^2_{K,T,\Gamma}}\right\} \times\frac{B_m(K^2,T,\Gamma)}{Q^2+\Pi(Q^2,T,\Gamma)}. \quad (45)$$

Because the fermion self-energy function has already been solved via Eq. (42), we can substitute it into Eq. (45), and then the equation can be solved using the iteration method. In Fig. 4, we display the momentum dependence of it for different impurity scattering rates Γ and numbers of fermion flavors N_f.

It can be seen that the derivation of the fermion self-energy function $B_m(P^2,T,\Gamma)$ is almost constant in the infrared

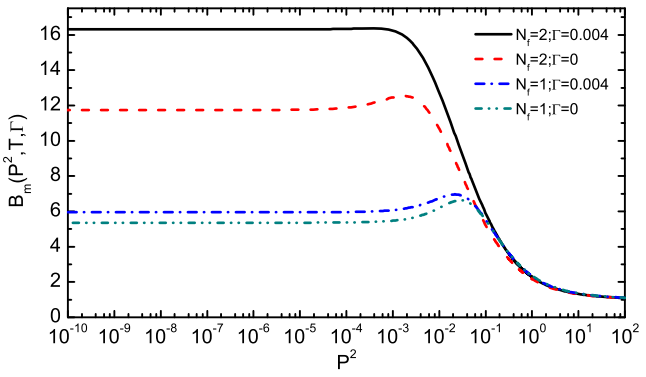

FIG. 4. Momentum dependence of the derivation of the fermion self-energy function $B_m(P^2,T,\Gamma)$ for different impurity scattering rates Γ and numbers of fermion flavors N_f at $T=10^{-3}$.

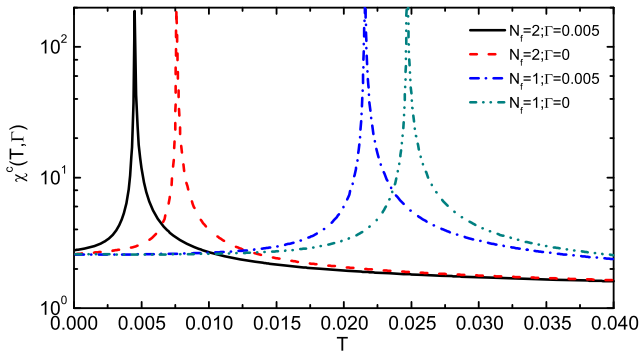

FIG. 5. Temperature dependence of the chiral susceptibility χ^c for different impurity scattering rates Γ and numbers of fermion flavors N_f.

region and approaches one in the ultraviolet region. For a given number of fermion flavors N_f, the infrared constant value of $B_m(P^2,T,\Gamma)$ increases as the impurity scattering rate Γ changes from zero to a finite value, while the ultraviolet $B_m(P^2,T,\Gamma)$ for different impurity scattering rates Γ are all close to zero. Furthermore, the function $B_m(P^2,T,\Gamma)$ rises as the number of fermion flavors N_f increases.

From Eqs. (42) and (45), we can calculate the chiral susceptibility. The temperature dependence of it for different impurity scattering rates Γ and numbers of fermion flavors N_f is shown in Fig. 5.

It is easy to see that the chiral susceptibility increases slowly with the temperature increasing and tends to divergence when the temperature approaches to the critical temperature T_c, which shows that the chiral phase transition driven by the temperature is a typical second-order phase transition. For a given number of fermion flavors N_f, the critical temperature T_c decreases when the impurity scattering rate Γ changes from zero to a finite value. This feature of the chiral susceptibility also means that impurity scattering plays the role of suppressing dynamical fermion mass generation. Moreover, when we enlarge the number of fermion flavors N_f, the critical temperature T_c decreases.

Similarly, for the thermal susceptibility, substituting Eq. (43) into Eq. (38) and performing the summation yield

$$\chi^T(T,\Gamma)=2\int\frac{d^2P}{(2\pi)^2}\left\{-B_T(P^2,T,\Gamma)\left[\frac{P^2\tanh\frac{\varepsilon_{P,T,\Gamma}}{2(T+c\Gamma)}}{\varepsilon^3_{P,T,\Gamma}}+\frac{B^2(P^2,T,\Gamma)\mathrm{sech}^2\frac{\varepsilon_{P,T,\Gamma}}{2(T+c\Gamma)}}{2(T+c\Gamma)\varepsilon^2_{P,T,\Gamma}}\right]+\frac{B(P^2,T,\Gamma)\mathrm{sech}^2\frac{\varepsilon_{P,T,\Gamma}}{2(T+c\Gamma)}}{2(T+c\Gamma)^2}\right\},\tag{46}$$

where the function $B_T(P^2,T,\Gamma)$ represents the derivative of fermion self-energy function with respect to the temperature and can be expressed as

$$B_T(P^2,T,\Gamma)=\int\frac{d^2K}{(2\pi)^2}\left\{B_T(K^2,T,\Gamma)\left[\frac{K^2\tanh\frac{\varepsilon_{K,T,\Gamma}}{2(T+c\Gamma)}}{\varepsilon^3_{K,T,\Gamma}}+\frac{B^2(K^2,T,\Gamma)\mathrm{sech}^2\frac{\varepsilon_{K,T,\Gamma}}{2(T+c\Gamma)}}{2(T+c\Gamma)\varepsilon^2_{K,T,\Gamma}}\right]-\frac{B(K^2,T,\Gamma)\mathrm{sech}^2\frac{\varepsilon_{K,T,\Gamma}}{2(T+c\Gamma)}}{2(T+c\Gamma)^2}-\frac{B(K^2,T,\Gamma)\tanh\frac{\varepsilon_{K,T,\Gamma}}{2(T+c\Gamma)}\Pi_T(Q^2,T,\Gamma)}{\varepsilon_{K,T,\Gamma}[Q^2+\Pi(Q^2,T,\Gamma)]}\right\}\times\frac{1}{Q^2+\Pi(Q^2,T,\Gamma)},\tag{47}$$

while the function $\Pi_T(Q^2,T,\Gamma)$ denotes the derivative of the boson polarization function with respect to the temperature, which can be obtained from Eq. (32):

$$\Pi_T(Q^2,T,\Gamma)=\frac{N_f}{\pi}\int_0^1 dx\left\{\ln\left[4\cosh^2\frac{\sqrt{x(1-x)}Q}{2(T+c\Gamma)}\right]-\frac{\sqrt{x(1-x)}Q\tanh\frac{\sqrt{x(1-x)}Q}{2T+c\Gamma}}{T+c\Gamma}\right\}.\tag{48}$$

Because the fermion self-energy function is known from Eq. (42), we substitute it into Eq. (47), and then the equation is solved by the iteration method. The momentum dependence of $-B_T(P^2,T,\Gamma)$, which is the negative of the derivation of the fermion self-energy function $B(P^2,T,\Gamma)$ with respect to the temperature, for different impurity scattering rates Γ and numbers of fermion flavors N_f is plotted in Fig. 6.

It can be seen that $-B_T(P^2,T,\Gamma)$ is almost constant in the infrared region and approaches zero in the ultraviolet region. For a given number of fermion flavors N_f, the

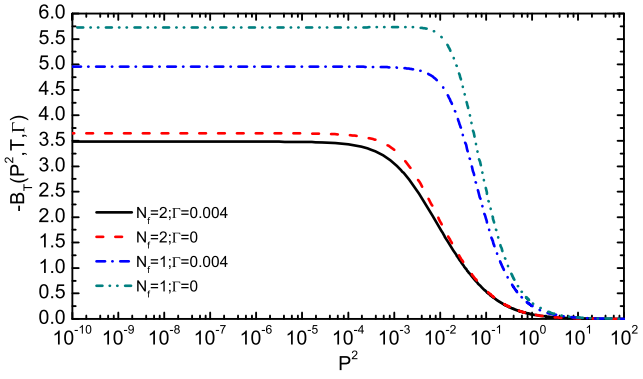

FIG. 6. Momentum dependence of $-B_T(P^2,T,\Gamma)$ for different impurity scattering rates Γ and numbers of fermion flavors N_f at $T=10^{-3}$.

infrared constant value of $-B_T(P^2,T,\Gamma)$ decreases as the impurity scattering rate Γ changes from zero to a finite value, while the ultraviolet $-B_T(P^2,T,\Gamma)$ for different impurity scattering rates Γ are all close to zero. Furthermore, the $-B_T(P^2,T,\Gamma)$ falls as the number of fermion flavors N_f increases.

From the two functions $B(P^2,T,\Gamma)$ and $B_T(P^2,T,\Gamma)$, we can obtain the dependence of the thermal susceptibility on the temperature. As a result, the behavior of the thermal susceptibility is plotted in Fig. 7.

We find that the thermal susceptibility increases slowly with the temperature increasing and then is close to divergence when the temperature arrives at the critical temperature T_c, which again reveals that the chiral phase transition is a typical second-order phase transition. For a given number of fermion flavors N_f, the critical temperature T_c decreases as the impurity scattering rate Γ changes from zero to a finite value. This feature of the thermal susceptibility means that impurity scattering suppresses the dynamical fermion mass generation. The critical temperature T_c also decreases when the number of fermion flavors N_f increases.

In order to investigate the relationship between the critical temperature T_c and the impurity scattering rate Γ, we calculate the chiral condensate, the chiral susceptibility, and the thermal susceptibility within a series of the impurity scattering rates Γ. In Fig. 8, the relationship between T_c and Γ is shown at the number of fermion flavors $N_f = 1$.

It can be clearly seen that there is a boundary that separates the $T_c - \Gamma$ plane into two regions. When the temperature and the impurity scattering rate Γ are both small, the system is in the phase of chiral symmetry breaking, while the system is in the phase of chiral symmetry restoration as the temperature and/or the impurity scattering rate Γ exceed the critical value. From the chiral condensate, the chiral susceptibility, and the thermal susceptibility, it is known that this transition of the system is a typical second-order phase transition.

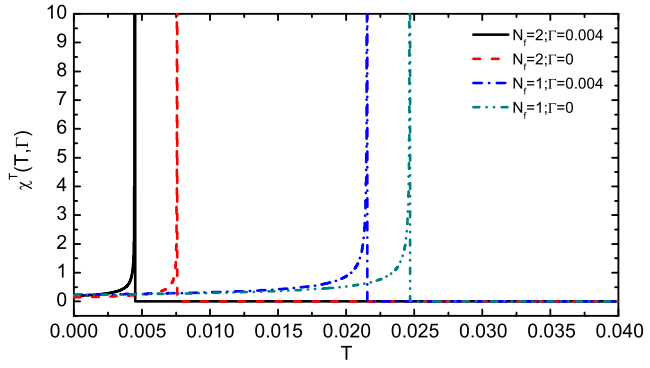

FIG. 7. Temperature dependence of the thermal susceptibility χ^T for different impurity scattering rates Γ and numbers of fermion flavors N_f.

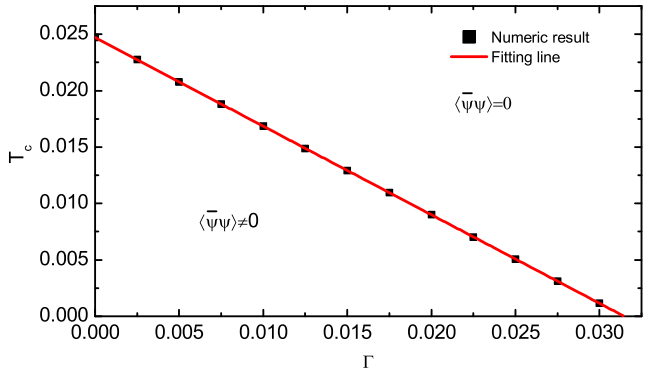

FIG. 8. Relationship between the critical temperature T_c and the impurity scattering rate Γ at the number of fermion flavors $N_f = 1$.

In addition, we can also find that the boundary is almost a straight line from Fig. 8. This feature of the boundary may be interpreted from Eqs. (32) and (42): the temperature and the impurity scattering rate Γ are combined in a linear way. The property of the equations determines that the relationship of the critical temperature T_c and impurity scattering rate Γ is also linear. For examining whether the interpretation is correct, we fit the result for the critical temperature T_c and corresponding impurity scattering rate Γ. It is found that they have the following relationship:

$$T_c = c_0 - c_1\Gamma, \tag{49}$$

where the constant c_0 is just equal to the critical temperature 2.47×10^{-2}, that is without the influences of impurity scattering, and the constant c_1 is almost equal to c appearing in Eqs. (32) and (42).

The phase diagram of $T_c - \Gamma$ at the number of fermion flavors $N_f = 2$ is also shown in Fig. 9. The qualitative behavior is similar to the case of $N_f = 1$ except for the quantitative value.

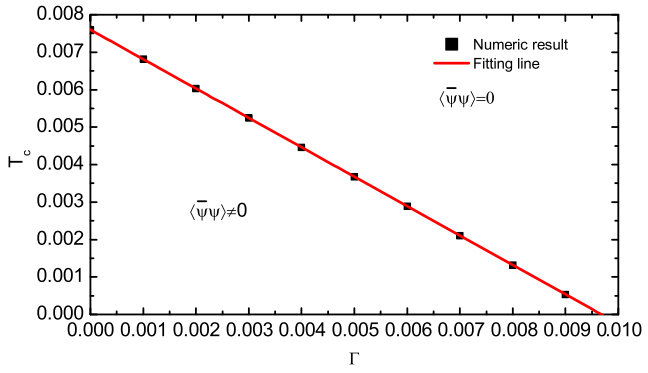

FIG. 9. Relationship between the critical temperature T_c and the impurity scattering rate Γ at the number of fermion flavors $N_f = 2$.

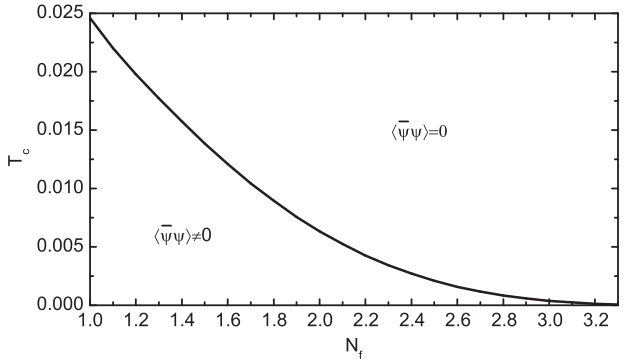

FIG. 10. Relationship between the critical temperature T_c and the number of fermion flavors N_f at the impurity scattering rate $\Gamma = 0$.

From the above discussions, it is found that, at the same value of the impurity scattering rate Γ, the critical temperature T_c decreases as the number of fermion flavors N_f increases. In order to confirm this conclusion, the chiral condensate and the two susceptibilities are calculated within a series of the numbers of fermion flavors N_f. Finally, at impurity scattering rate $\Gamma = 0$, we show the relationship between T_c and N_f in Fig. 10.

From Fig. 10, it can be found that the value of the critical number of fermion flavors N_f^c, where the critical temperature T_c is equal to zero, is 3.3 that is close to the result obtained by employing the large-N_f approximation of the DSEs at zero temperature [37], and the critical temperature T_c decreases as the number of fermion flavors N_f increases (or, equivalently, the critical number of fermion flavors N_f^c decreases with the temperature increasing). There is a boundary, such that for (N_f, T_c) below this boundary $\langle\bar{\psi}\psi\rangle \neq 0$, and for ($N_f$,$T_c$) above it $\langle\bar{\psi}\psi\rangle = 0$. In addition, because the effect of impurity scattering is to replace the temperature T with the linear combination of temperature T and impurity scattering rate Γ when the analytic approximations to the Γ function and ψ function appearing in Eq. (29) are adopted, the critical number of fermion flavors N_f^c also decreases as the impurity scattering rate Γ increases for a given temperature.

V. SUMMARY AND CONCLUSIONS

In this paper, the influences of finite temperature and impurity scattering on the chiral phase transition in QED_3 are investigated. Within the Born approximation, the effects of impurity scattering are treated by introducing a damping term in the energy component of the fermion propagator.

First we numerically solve the DSEs for the fermion and boson propagators to the leading order in the $1/N_f$ expansion at zero frequency and discuss the momentum dependence of the fermion self-energy function $B(P^2)$ for different impurity scattering rates Γ and the numbers of fermion flavors N_f at a given temperature.

Then we calculate the chiral condensate, the chiral susceptibility, and the thermal susceptibility within a range of the impurity scattering rates Γ and the numbers of fermion flavors N_f. The results show that, for a given number of fermion flavors N_f and impurity scattering rate Γ, the chiral condensate decreases slowly and the two susceptibilities increase gradually as the temperature increases; when the temperature arrives at the critical value T_c, the chiral condensate decreases rapidly to zero; meanwhile, the two susceptibilities tend to divergence, which signals a typical second-order phase transition. For a given number of fermion flavors N_f, the critical temperature T_c decreases when the impurity scattering rate Γ increases, which indicates that impurity scattering plays a role of suppressing the dynamical fermion mass generation.

Finally, we discuss the relationship among the critical temperature T_c, the impurity scattering rate Γ, and the number of fermion flavors N_f and find that T_c decreases as Γ (or N_f) increases, which indicates that there is a boundary that separates the $T_c - \Gamma$ (or $T_c - N_f$) plane into chiral symmetry breaking and chiral symmetry restoration regions.

ACKNOWLEDGMENTS

We express our appreciation to C. D. Roberts, Q. H. Wang, and J. R. Wang for helpful discussions. This work is supported in part by the National Natural Science Foundation of China (under Grants No. 11275097, No. 11475085, and No. 11535005) and the National Basic Research Program of China (under Grant No. 2012CB921504).

APPENDIX A: CALCULATIONS OF POLARIZATION FUNCTIONS

To the leading order in $1/N_f$ expansion, the one-loop contribution to the vacuum polarization tensor is given by

$$\Pi_{\mu\nu}(q) = -N_f T \sum\!\!\!\!\!\!\int \mathrm{Tr}[\gamma_\mu S_0(k)\gamma_\nu S_0(p)], \quad \text{(A1)}$$

where $p = k + q$, and the free fermion propagator reads

$$S_0^{-1}(k) = i\gamma_\mu k_\mu = i\vec{\gamma}\cdot\vec{k} + i\gamma_3 k_3. \quad \text{(A2)}$$

Substituting Eq. (A2) into Eq. (A1), we can obtain

$$\begin{aligned}\Pi_{\mu\nu}(q) &= -N_f T \sum\!\!\!\!\!\!\int \mathrm{Tr}\left[\gamma_\mu \frac{1}{i\gamma_\rho k_\rho}\gamma_\nu \frac{1}{i\gamma_\sigma (k+q)_\sigma}\right] \\ &= N_f T \sum\!\!\!\!\!\!\int \mathrm{Tr}\frac{\gamma_\mu\gamma_\rho k_\rho \gamma_\nu \gamma_\sigma (k+q)_\sigma}{k^2(k+q)^2} \\ &= 4N_f T \sum\!\!\!\!\!\!\int \frac{\mathcal{I}^1_{\mu\nu}}{k^2(k+q)^2}, \end{aligned} \quad \text{(A3)}$$

where $\mathcal{I}^1_{\mu\nu} = 2k_\mu k_\nu + k_\mu q_\nu + k_\nu q_\mu - k(k+q)\delta_{\mu\nu}$.

With the help of the Feynman parametrization formula

$$\frac{1}{AB}=\int_0^1 \mathrm{d}x \frac{1}{[xA+(1-x)B]^2}, \tag{A4}$$

Eq. (A3) can be expressed as

$$\Pi_{\mu\nu}(q)=4N_f T\int_0^1 \mathrm{d}x \sum\!\!\!\!\!\!\int \frac{\mathcal{I}^1_{\mu\nu}}{[(k+xq)^2+x(1-x)q^2]^2}. \tag{A5}$$

Defining a shifted three-momentum by $l=k+xq$ and changing variables in the momentum integral give

$$\Pi_{\mu\nu}(q)=4N_f T\int_0^1 \mathrm{d}x \sum\!\!\!\!\!\!\int \frac{\mathcal{I}^2_{\mu\nu}}{[l^2+x(1-x)q^2]^2}, \tag{A6}$$

where

$$\mathcal{I}^2_{\mu\nu}=2l_\mu l_\nu+(1-2x)(l_\mu q_\nu+l_\nu q_\mu-l\cdot q\delta_{\mu\nu}) +2x(1-x)(q^2\delta_{\mu\nu}-q_\mu q_\nu)-[l^2+x(1-x)q^2]\delta_{\mu\nu}. \tag{A7}$$

The temporal component of vacuum polarization tensor is written as

$$\Pi_{33}(q)=4N_f T\int_0^1 \mathrm{d}x\int\frac{\mathrm{d}^2L}{(2\pi)^2}[S_1-2(L^2+x(1-x)q_0^2)S_2 +(1-2x)q_0 S^*], \tag{A8}$$

with

$$S_i=\sum_{n=-\infty}^{+\infty}\frac{1}{[l_0^2+L^2+x(1-x)q^2]^i} \tag{A9}$$

and

$$S^*=\sum_{n=-\infty}^{+\infty}\frac{l_3}{[l_0^2+L^2+x(1-x)q^2]^2}. \tag{A10}$$

Within the instantaneous exchange approximation $q_0=0$, Eq. (A8) reduces to

$$\Pi_{33}(Q,T)=4N_f T\int_0^1 \mathrm{d}x\int\frac{\mathrm{d}^2L}{(2\pi)^2}[S_1-2L^2S_2], \tag{A11}$$

with

$$\begin{aligned}S_i&=\sum_{n=-\infty}^{+\infty}\frac{1}{[k_3^2+L^2+x(1-x)Q^2]^i}\\&=\sum_{n=-\infty}^{+\infty}\frac{1}{[((2n+1)\pi T)^2+L^2+x(1-x)Q^2]^i}\\&=\left(\frac{1}{2\pi T}\right)^{2i}\sum_{n=-\infty}^{+\infty}\frac{1}{[(n+\frac{1}{2})^2+Y^2]^i},\end{aligned} \tag{A12}$$

where $Y=\frac{\sqrt{L^2+x(1-x)Q^2}}{2\pi T}$.

After summing over n, S_1 can be written as

$$S_1=\frac{1}{4\pi T^2 Y}\tanh\pi Y, \tag{A13}$$

and S_2 is associated with S_1 by the following relationship:

$$\begin{aligned}S_2&=-\frac{1}{8\pi^2T^2Y}\frac{\partial S_1}{\partial Y}\\&=\frac{1}{32\pi^2T^4Y^2}\left(\frac{\tanh\pi Y}{\pi Y}-\mathrm{sech}^2\pi Y\right).\end{aligned} \tag{A14}$$

Substituting Eqs. (A13) and (A14) into Eq. (A11) and performing the integral over L, we obtain the following expression for the temporal component of the vacuum polarization tensor:

$$\Pi(Q^2,T)=\frac{2N_fT}{\pi}\int_0^1 \mathrm{d}x\ln\left[2\cosh\frac{\sqrt{x(1-x)}Q}{2T}\right]. \tag{A15}$$

APPENDIX B: CALCULATIONS OF POLARIZATION FUNCTIONS IN THE PRESENCE OF IMPURITY SCATTERING

The one-loop contribution to the vacuum polarization tensor including impurity scattering can be written as

$$\Pi_{\mu\nu}(q,\Gamma)=-N_f T\sum\!\!\!\!\!\!\int \mathrm{Tr}[\gamma_\mu S_0(k,\Gamma)\gamma_\nu S_0(p,\Gamma)], \tag{B1}$$

where the free fermion propagator in the presence of impurity scattering is given by

$$S_0^{-1}(k,\Gamma)=i\gamma_\mu k_{\mu,\Gamma}=i\vec{\gamma}\cdot\vec{k}+i\gamma_3 k_{3,\Gamma}, \tag{B2}$$

with $k_{3,\Gamma}=k_3+\Gamma\mathrm{sgn}(k_3)$

Substituting Eq. (B2) into Eq. (B1), we arrive at

$$\begin{aligned}\Pi_{\mu\nu}(q,\Gamma) &= -N_f T \sum\!\!\!\!\!\!\int \mathrm{Tr}\left[\gamma_\mu \frac{1}{i\gamma_\rho k_{\rho,\Gamma}} \gamma_\nu \frac{1}{i\gamma_\sigma (k+q)_{\sigma,\Gamma}}\right] \\ &= N_f T \sum\!\!\!\!\!\!\int \mathrm{Tr}\frac{\gamma_\mu\gamma_\rho k_{\rho,\Gamma}\gamma_\nu\gamma_\sigma (k+q)_{\sigma,\Gamma}}{k_\Gamma^2 (k+q)_\Gamma^2} \\ &= 4N_f T \sum\!\!\!\!\!\!\int \frac{\mathcal{I}^3_{\mu\nu}}{k_\Gamma^2 (k+q)_\Gamma^2}, \end{aligned} \tag{B3}$$

where
$\mathcal{I}^3_{\mu\nu} = k_{\mu,\Gamma}(k+q)_{\nu,\Gamma} + k_{\nu,\Gamma}(k+q)_{\mu,\Gamma} - k_\Gamma (k+q)_\Gamma \delta_{\mu\nu}$.

Using the Feynman parametrization formula and employing a shifted three-momentum $l_{\mu,\Gamma} = k_{\mu,\Gamma} + x q_\mu$, Eq. (B3) can be written as

$$\Pi_{\mu\nu}(q,\Gamma) = \int_0^1 \mathrm{d}x \sum\!\!\!\!\!\!\int \frac{4N_f T \mathcal{I}^4_{\mu\nu}}{[l_\Gamma^2 + x(1-x)q^2 + 2x(k_3+q_3)\delta]^2}, \tag{B4}$$

where

$$\begin{aligned}\mathcal{I}^4_{\mu\nu} &= 2l_{\mu,\Gamma} l_{\nu,\Gamma} + (1-2x)(l_{\mu,\Gamma} q_\nu + l_{\nu,\Gamma} q_\mu - l_\Gamma \cdot q \delta_{\mu\nu}) \\ &\quad + 2x(1-x)(q^2\delta_{\mu\nu} - q_\mu q_\nu) - [l_\Gamma^2 + x(1-x)q^2]\delta_{\mu\nu} \\ &\quad + [(l_{\mu,\Gamma} - x q_\mu)\delta_{\nu,3} + (l_{\nu,\Gamma} - x q_\nu)\delta_{\mu,3} \\ &\quad - (l_{3,\Gamma} - x q_3)\delta_{\mu\nu}]\delta. \end{aligned} \tag{B5}$$

The temporal component of the vacuum polarization tensor including impurity scattering is expressed as

$$\Pi_{33}(q,\Gamma) = 4N_f T \int_0^1 \mathrm{d}x \int \frac{\mathrm{d}^2 L}{(2\pi)^2} \left\{ S_1 - 2\left[L^2 + x(1-x)q_0^2 + x\left(k_3 + \frac{3}{2}q_3\right)\delta\right] S_2 + [(1-2x)q_3 + \delta] S^* \right\}, \tag{B6}$$

with

$$S_i = \sum_{n=-\infty}^{+\infty} \frac{1}{[l_{3,\Gamma}^2 + L^2 + x(1-x)q^2 + 2x(k_3+q_3)\delta]^i} \tag{B7}$$

and

$$S^* = \sum_{n=-\infty}^{+\infty} \frac{l_{3,\Gamma}}{[l_{3,\Gamma}^2 + L^2 + x(1-x)q^2 + 2x(k_3+q_3)\delta]^2}. \tag{B8}$$

Within the instantaneous exchange approximation $q_0 = 0$, we are left with

$$\Pi_{33}(Q,T,\Gamma) = 4N_f T \int_0^1 \mathrm{d}x \int \frac{\mathrm{d}^2 L}{(2\pi)^2} [S_1 - 2L^2 S_2]. \tag{B9}$$

Meanwhile,

$$\begin{aligned} S_i &= \sum_{n=-\infty}^{+\infty} \frac{1}{[(k_3 + \Gamma \mathrm{sgn}(k_3))^2 + L^2 + x(1-x)Q^2]^i} \\ &= \sum_{n=-\infty}^{+\infty} \frac{1}{[((2n+1)\pi T + \Gamma \mathrm{sgn}((2n+1)\pi T))^2 + (2\pi T Y)^2]^i} \\ &= \left(\frac{1}{2\pi T}\right)^{2i} \sum_{n=-\infty}^{+\infty} \frac{1}{[(n+\frac{1}{2} + \frac{\Gamma}{2\pi T}\mathrm{sgn}((n+\frac{1}{2}))^2 + Y^2]^i}. \end{aligned} \tag{B10}$$

Performing the summation over n yields

$$S_1 = \frac{1}{2\pi^2 T^2 Y} \mathrm{Im}\left[\psi\left(\frac{1}{2} + \frac{\Gamma}{2\pi T} + i\frac{Y}{2\pi T}\right)\right] \tag{B11}$$

and

$$\begin{aligned} S_2 &= -\frac{1}{8\pi^2 T^2 Y}\frac{\partial S_1}{\partial Y} \\ &= \frac{1}{16\pi^4 T^4 Y^3} \mathrm{Im}\left[\psi\left(\frac{1}{2} + \frac{\Gamma}{2\pi T} + i\frac{Y}{2\pi T}\right)\right] \\ &\quad + \frac{1}{16\pi^4 T^4 Y^2} \frac{\partial \mathrm{Im}[\psi(\frac{1}{2} + \frac{\Gamma}{2\pi T} + i\frac{Y}{2\pi T})]}{\partial Y}. \end{aligned} \tag{B12}$$

Substituting Eqs. (B11) and (B12) into Eq. (B9) and performing the integral over L, we finally obtain the expression for the temporal component of the vacuum polarization tensor including impurity scattering:

$$\begin{aligned} \Pi(Q^2,T,\Gamma) = \frac{4N_f T}{\pi} \int_0^1 \mathrm{d}x \Bigg\{ &\mathrm{Re}\left[\ln\Gamma\left(\frac{1}{2} + \frac{\Gamma + iX}{2\pi T}\right)\right] \\ &+ \frac{X^2 - C^2}{X^2} \mathrm{Im}\left[\psi\left(\frac{1}{2} + \frac{\Gamma + iX}{2\pi T}\right)\right]\Bigg\}\Bigg|_C^\infty, \end{aligned} \tag{B13}$$

where $C = \sqrt{x(1-x)}Q$.

[1] M. A. Halasz, A. D. Jackson, R. E. Shrock, M. A. Stephanov, and J. J. M. Verbaarschot, Phys. Rev. D **58**, 096007 (1998).
[2] D. T. Son and M. A. Stephanov, Phys. Rev. Lett. **86**, 592 (2001).
[3] P. de Forcrand and O. Philipsen, Nucl. Phys. **B673**, 170 (2003).
[4] M. Buballa, Phys. Rep. **407**, 205 (2005).
[5] A. Andronic, P. Braun-Munzinger, and J. Stachel, Nucl. Phys. **A772**, 167 (2006).
[6] Y. Aoki, G. Endrő di, Z. Fodor, S. D. Katz, and K. K. Szabó, Nature (London) **443**, 675 (2006).
[7] M. G. Alford, A. Schmitt, K. Rajagopal, and T. Schäfer, Rev. Mod. Phys. **80**, 1455 (2008).
[8] K. Fukushima and T. Hatsuda, Rep. Prog. Phys. **74**, 014001 (2011).
[9] A. Bazavov *et al.*, Phys. Rev. D **85**, 054503 (2012).
[10] A. Ohnishi, Prog. Theor. Phys. Suppl. **193**, 1 (2012).
[11] Z. F. Cui, C. Shi, Y. H. Xia, Y. Jiang, and H. S. Zong, Eur. Phys. J. C **73**, 2612 (2013).
[12] S. S. Xu, Z. F. Cui, B. Wang, Y. M. Shi, Y. C. Yang, and H. S. Zong, Phys. Rev. D **91**, 056003 (2015).
[13] T. W. Appelquist, M. Bowick, D. Karabali, and L. C. R. Wijewardhana, Phys. Rev. D **33**, 3704 (1986).
[14] K.-I. Kondo and H. Nakatani, Prog. Theor. Phys. **87**, 193 (1992).
[15] K.-I. Kondo, Phys. Rev. D **55**, 7826 (1997).
[16] K.-I. Kondo and T. Murakami, Phys. Lett. B **410**, 257 (1997).
[17] K.-I. Kubota and H. Terao, Prog. Theor. Phys. **105**, 809 (2001).
[18] B. Svetitsky, O. Raviv, and Y. Shamir, Proc. Sci., LATTICE2014 (**2014**) 051 [arXiv:1410.0118].
[19] M. Pennington and D. Walsh, Phys. Lett. B **253**, 246 (1991).
[20] D. Curtis, M. Pennington, and D. Walsh, Phys. Lett. B **295**, 313 (1992).
[21] I. Aitchison, N. Dorey, M. Klein-Kreisler, and N. Mavromatos, Phys. Lett. B **294**, 91 (1992).
[22] C. D. Roberts and A. G. Williams, Prog. Part. Nucl. Phys. **33**, 477 (1994).
[23] D. J. Lee, Phys. Rev. D **58**, 105012 (1998); D. Lee and G. Metikas, Int. J. Mod. Phys. A **14**, 2921 (1999).
[24] G. Triantaphyllou, Phys. Rev. D **58**, 065006 (1998); J. High Energy Phys. 03 (1999) 020.
[25] V. P. Gusynin and M. Reenders, Phys. Rev. D **68**, 025017 (2003).
[26] M. He, H. T. Feng, W. M. Sun, and H. S. Zong, Mod. Phys. Lett. A **22**, 449 (2007).
[27] W. Li and G. Z. Liu, Phys. Rev. D **81**, 045006 (2010).
[28] A. Bashir, A. Raya, and S. Sánchez-Madrigal, Phys. Rev. D **84**, 036013 (2011).
[29] H. T. Feng, S. Shi, P. L. Yin, and H. S. Zong, Phys. Rev. D **86**, 065002 (2012).
[30] P. L. Yin, Z. F. Cui, H. T. Feng, and H. S. Zong, Ann. Phys. (Amsterdam) **348**, 306 (2014).
[31] J. R. Wang, G. Z. Liu, and C. J. Zhang, Phys. Rev. D **91**, 045006 (2015).
[32] C. J. Burden, J. Praschifka, and C. D. Roberts, Phys. Rev. D **46**, 2695 (1992).
[33] P. Maris, Phys. Rev. D **52**, 6087 (1995).
[34] Y. Hoshino, J. High Energy Phys. 09 (2004) 048.
[35] G. Z. Liu, H. Jiang, W. Li, and G. Cheng, Phys. Rev. B **79**, 014507 (2009).
[36] J. Wang, J. R. Wang, W. Li, and G. Z. Liu, Phys. Rev. D **82**, 067701 (2010).
[37] T. Appelquist, D. Nash, and L. C. R. Wijewardhana, Phys. Rev. Lett. **60**, 2575 (1988).
[38] D. Nash, Phys. Rev. Lett. **62**, 3024 (1989).
[39] P. Maris, Phys. Rev. D **54**, 4049 (1996).
[40] C. S. Fischer, R. Alkofer, T. Dahm, and P. Maris, Phys. Rev. D **70**, 073007 (2004).
[41] A. Bashir, A. Raya, I. C. Cloët, and C. D. Roberts, Phys. Rev. C **78**, 055201 (2008); A. Bashir, A. Raya, S. Snchez-Madrigal, and C. Roberts, Few-Body Syst. **46**, 229 (2009).
[42] J. Braun, H. Gies, L. Janssen, and D. Roscher, Phys. Rev. D **90**, 036002 (2014).
[43] N. Dorey and N. Mavromatos, Phys. Lett. B **266**, 163 (1991); Nucl. Phys. **B386**, 614 (1992).
[44] I. J. R. Aitchison and M. Klein-Kreisler, Phys. Rev. D **50**, 1068 (1994).
[45] H. T. Feng, S. Shi, W. M. Sun, and H. S. Zong, Phys. Rev. D **86**, 045020 (2012).
[46] P. M. Lo and E. S. Swanson, Phys. Lett. B **697**, 164 (2011); Phys. Rev. D **89**, 025015 (2014).
[47] D. H. Kim, P. A. Lee, and X.-G. Wen, Phys. Rev. Lett. **79**, 2109 (1997).
[48] D. H. Kim and P. A. Lee, Ann. Phys. (N.Y.) **272**, 130 (1999).
[49] W. Rantner and X. G. Wen, Phys. Rev. Lett. **86**, 3871 (2001); Phys. Rev. B **66**, 144501 (2002).
[50] M. Franz and Z. Tešanović, Phys. Rev. Lett. **87**, 257003 (2001); M. Franz, Z. Tešanovicć, and O. Vafek, Phys. Rev. B **66**, 054535 (2002); Z. Tešanovicć, O. Vafek, and M. Franz, Phys. Rev. B **65**, 180511 (2002).
[51] I. F. Herbut, Phys. Rev. Lett. **88**, 047006 (2002); Phys. Rev. B **66**, 094504 (2002).
[52] G. Z. Liu and G. Cheng, Phys. Rev. B **66**, 100505 (2002).
[53] P. A. Lee, N. Nagaosa, and X. G. Wen, Rev. Mod. Phys. **78**, 17 (2006).
[54] S. G. Sharapov, V. P. Gusynin, and H. Beck, Phys. Rev. B **69**, 075104 (2004).
[55] V. P. Gusynin, S. G. Sharapov, and J. P. Carbotte, Int. J. Mod. Phys. B **21**, 4611 (2007).
[56] M. d. J. Anguiano and A. Bashir, Few-Body Syst. **37**, 71 (2005).
[57] A. Raya and E. D. Reyes, J. Phys. A **41**, 355401 (2008).
[58] O. K. Kalashnikov, Pis'ma Zh. Eksp. Teor. Fiz. **41**, 477 (1985) [JETP Lett. **41**, 582 (1985)].
[59] C. D. Roberts and S. M. Schmidt, Prog. Part. Nucl. Phys. **45**, S1 (2000).
[60] J. Rusnak and R. Furnstahl, Z. Phys. A **352**, 345 (1995).
[61] M. Harada and A. Shibata, Phys. Rev. D **59**, 014010 (1998).
[62] M. Carrington, W. Chen, and R. Kobes, Eur. Phys. J. C **18**, 757 (2001).
[63] E. V. Gorbar, V. P. Gusynin, V. A. Miransky, and I. A. Shovkovy, Phys. Rev. B **66**, 045108 (2002).
[64] R. Dillenschneider and J. Richert, Phys. Rev. B **73**, 224443 (2006).
[65] A. Altland and B. D. Simons, *Condensed Matter Field Theory* (Cambridge University Press, Cambridge, England, 2006).

[66] F. Karsch and E. Laermann, Phys. Rev. D **50**, 6954 (1994).
[67] K. Fukushima, Phys. Lett. B **591**, 277 (2004).
[68] H. S. Zong, F. Y. Hou, W. M. Sun, J. L. Ping, and E. G. Zhao, Phys. Rev. C **72**, 035202 (2005).
[69] D. Blaschke, A. Höll, C. D. Roberts, and S. Schmidt, Phys. Rev. C **58**, 1758 (1998).
[70] K. Morita, V. Skokov, B. Friman, and K. Redlich, Phys. Rev. D **84**, 074020 (2011).
[71] V. Skokov, Phys. Rev. D **85**, 034026 (2012).
[72] S. Shi, Y. C. Yang, Y. H. Xia, Z. F. Cui, X. J. Liu, and H. S. Zong, Phys. Rev. D **91**, 036006 (2015).
[73] S. Coleman, Commun. Math. Phys. **31**, 259 (1973).
[74] N. D. Mermin and H. Wagner, Phys. Rev. Lett. **17**, 1133 (1966).
[75] D. J. Gross and A. Neveu, Phys. Rev. D **10**, 3235 (1974).
[76] B. Rosenstein, B. J. Warr, and S. H. Park, Phys. Rep. **205**, 59 (1991).